

Observation of Anomalous Phonon Softening in Bilayer Graphene

Jun Yan^{1,*}, Erik A. Henriksen¹, Philip Kim¹, and Aron Pinczuk^{1,2}
¹*Department of Physics, Columbia University, New York, NY 10027, USA*
²*Department of Applied Physics and Applied Mathematics, Columbia University, New York, NY 10027, USA*

The interaction of electron-hole pairs with lattice vibrations exhibits a wealth of intriguing physical phenomena. The Kohn anomaly is a renowned example where electron-phonon coupling leads to non-analytic phonon dispersion at specific momentum nesting the Fermi surface [1]. Here we report evidence of another type of phonon anomaly discovered by low temperature Raman spectroscopy in bilayer graphene where the charge density is modulated by the electric field effect. This anomaly, arising from charge-tunable modulations of particle-hole pairs that are resonantly coupled to lattice vibrations, is predicted to exhibit a logarithmic divergence in the long-wavelength optical-phonon energy. In a non-uniform bilayer of graphene, the logarithmic divergence is abated by charge density inhomogeneity leaving as a vestige an anomalous phonon softening. The observed softening marks the first confirmation of the phonon anomaly as a key signature of the resonant deformation-potential electron-phonon coupling. The high sensitivity of the phonon softening to charge density non-uniformity creates significant venues to explore the interplay between fundamental interactions and disorder in the atomic layers.

Recently, the ability to use the electric field effect (EFE) to continuously dope large densities of electrons or holes into graphene [2] has led to general interest in the deformation potential coupling of optical phonons with charge carriers in the extreme two-dimensional(2D) atomic limit [3, 4, 5, 6, 7], and to experimental observations of charge-tunable phonon energy and lifetime in single layer graphene [8, 9, 10]. In prior EFE-Raman experiments, however, a logarithmically-divergent phonon-energy anomaly[3] predicted by the dynamical perturbation theory was not observed. The puzzling absence of the phonon anomaly was attributed to the presence of large non-uniformity of the charge density in monolayer graphene samples [8]. This interpretation is subsequently supported by the observation of asymmetric phonon line-shape in the EFE-Raman spectra at low doping levels[11].

In this paper we demonstrate that the phonon anomaly, while proposed initially in single layer graphene [3], is a generic feature of tunable resonant electron-phonon coupling when the particle-hole pair energy is close to the phonon energy (Fig.1). We report experimental observation of the anomalous phonon softening, a clear signature of such phonon anomaly, in bilayer graphene. The observation of the resonant phonon softening is facilitated in bilayer graphene. The reason is that

the coupling between the two graphene layers results in a nearly parabolic dispersion and relatively large density of states near the vanishing band gap, making the phonon anomaly robust even in the presence of relatively large charge density non-uniformity.

Rather than being a special property unique to the monolayer graphene, the anomaly is anticipated to occur in any multi-band electron system where the zero momentum optical phonon can create resonant electron-hole pairs across the conduction and valence bands. Figure 1 illustrates the concept of the phonon anomaly in a 2D gapless semiconductor with particle-hole symmetry as a model system. A system with similar low energy band structure is in fact bilayer graphene, in which the two valleys of conduction and valence bands are centered at K and K' corner points of the Brillouin zone [12]. The deformation-potential interaction couples vertical electron-hole interband excitations with long-wavelength optical phonons in graphene [13, 14]. This coupling contributes to the renormalization of the phonon energy [15]. Considering the electron-phonon interaction within 2nd order time-dependent perturbation theory [15], combined with the Pauli exclusion principle, we obtain the change of phonon energy ω_{ph} with tuning of the Fermi energy E_F :

$$\hbar\omega_{ph}(E_F) - \hbar\omega_{ph}(E_F = 0) \sim -\lambda \int_0^{2|E_F|} dE_{e-h} \frac{2E_{e-h}}{\hbar\omega_{ph}^2 - E_{e-h}^2} \sim \lambda \ln \left| 1 - \frac{2|E_F|}{\hbar\omega_{ph}} \right| \quad (1)$$

where E_{e-h} is the energy of an electron-hole pair, λ is the electron-phonon coupling parameter with dimension of energy. Because of the resonant denominator

$\frac{1}{\hbar\omega_{ph}^2 - E_{e-h}^2}$ in equation (1), the perturbative contributions to ω_{ph} have a sign change at $E_{e-h} = \hbar\omega_{ph}$ and are

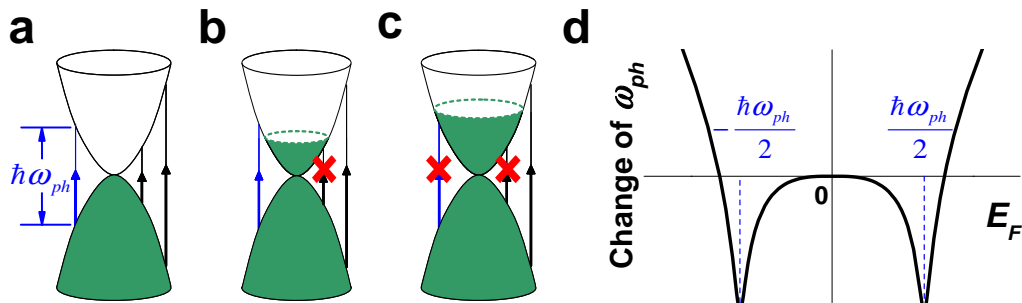


FIG. 1: **Illustration of the phonon anomaly concept.** **a-c**, Vertical interband electron-hole pair transitions in a gapless 2D semiconductor with 3 different Fermi levels. Regions with green shading are filled with electrons. The transition indicated by the blue arrow is the resonance with the long-wavelength optical phonon. **d**, Predicted change of phonon energy as a function of the Fermi energy. The two phonon anomalies show up at $E_F = \pm \hbar\omega_{ph}/2$.

markedly enhanced near the resonance (the interband transition indicated with a blue arrow in Fig. 1a). When $|E_F|$ is increased, the positive and negative enhanced perturbations to ω_{ph} are switched off due to restrictions placed by the Pauli Principle (illustrations for the case of electron doping are shown in Fig. 1b,c). For this reason, the modulation of carrier density in the system results in marked changes in the optical phonon energy around $|E_F| = \hbar\omega_{ph}/2$, as shown in Fig. 1d.

Note that in the derivation of equation (1), no assumptions of system dimensionality or band dispersion curvature were made. We expect the phonon anomaly in principle to show up in 1D system like metallic or near zero gap semiconducting carbon nanotubes [16, 17], graphene nanoribbons [18], 2D system like graphene thin films, 3D system like silicon and germanium [19, 20]. In fact, like in single layer graphene, similar log-divergence was predicted, albeit not observed, in the studies of chemically doped silicon [19].

In the present work, we use EFE to tune E_F to access the resonant electron-phonon interaction condition of the phonon anomaly in bilayer graphene. Low temperature Raman spectroscopy was employed to detect the evolution of the zero momentum optical phonon, known as G band in graphite and graphene thin films. Its energy $\hbar\omega_G \approx 1580 \text{ cm}^{-1} \approx 196 \text{ meV}$. Bilayer graphene is an intriguing electronic system in which transport measurements have revealed unconventional quantum Hall effect and Berry's phase of 2π [21]. It has 4 carbon atoms in its unit cell. The locations of them are A_t , B_t in the top layer, A_b , B_b in the bottom layer (Fig. 2a). The p_z orbital of these atoms forms 4 π bands in Fig. 2b.

Figure 2c schematically shows our experimental setup. A back gate voltage V_g is applied across a thin layer of SiO_2 dielectric sandwiched by bilayer graphene and doped silicon to induce charge carriers in the sample. The gating efficiency is about $7.2 \times 10^{10} \text{ cm}^{-2}/\text{Volt}$ [22]. For Stokes Raman scattering, $\omega_{Stokes} = \omega_L - \omega_S$, where ω_L and ω_S are frequencies of the incident and scattered light, respectively. The experiment is performed with the

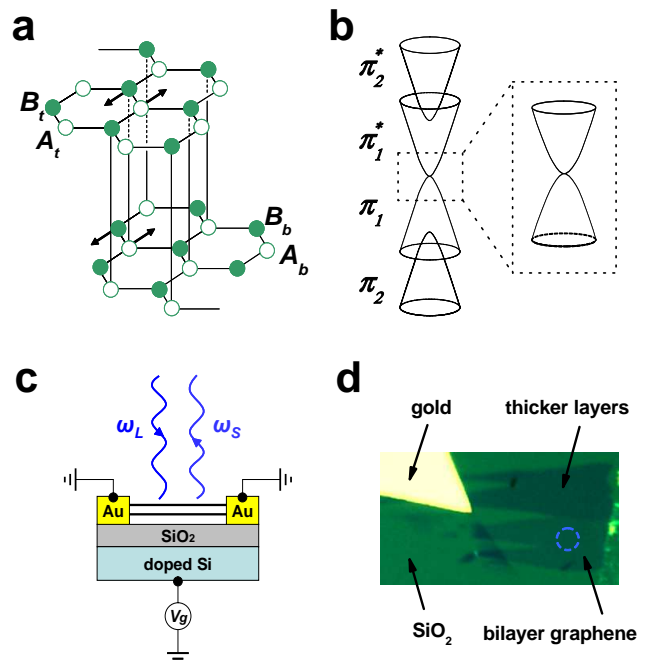


FIG. 2: **Bilayer graphene and the EFE-Raman setup.** **a**, Bilayer graphene lattice with 4 carbon atoms A_t , B_t , A_b , B_b in its unit cell. Black arrows indicate carbon atom motion in the G band lattice vibration. **b**, π bands of bilayer graphene near the K and K' corner points of the Brillouin zone. The low energy region is zoomed out to illustrate that the dispersion is drastically different from single layer graphene [12]. **c**, Schematic drawing of the experimental setup. The two black lines in-between the gold contacts represent bilayer graphene. **d**, Optical image of the bilayer graphene device. The dashed blue circle is the position of the laser spot.

sample mounted inside a variable temperature cryostat with optical access. Data shown in this work are taken at 12 K.

The evolution of bilayer G band with the gate voltage V_g is displayed in Fig. 3. The EFE induced changes in the spectra are nearly symmetric about $V_g = 10\text{V}$ (Fig. 3a). As in single layer graphene [8], this symmetry, which

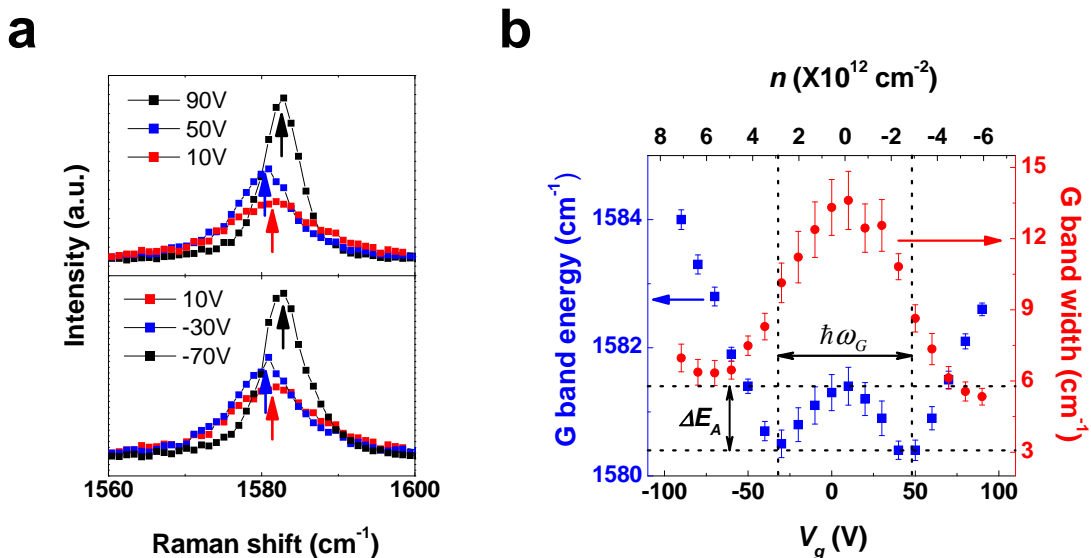


FIG. 3: **Evolution of the G band of bilayer graphene with charge doping.** **a**, G band at 5 different gate voltages. The arrows indicate the phonon peak positions. Spectra were taken at 12K in Helium gas environment. **b**, Energy and line-width of G band extracted from spectra in panel a. Two phonon anomalies are clearly resolved in the phonon energy evolution (blue squares).

determines the charge-neutral point of the sample, reflects the underlying particle-hole symmetry in the band structure of bilayer graphene. Another important feature in the data is that, the phonon bands have smaller line width at large charge doping with electrons or holes, indicating longer lifetime. This change of width is due to Landau damping of the G-phonon into electron-hole pairs when $|E_F| < \hbar\omega_G/2$ at small charge doping. Similar effects were observed in EFE tuned Raman spectra in single layer graphene [8].

While the observed G phonon line width evolution in bilayer is similar to that of a single layer, changes in the phonon energy are drastically different. In single layer graphene, G phonon frequency exhibits only one minimum as the EFE tuned charge density n passes through the charge-neutral Dirac point, and the phonon monotonically stiffens with increasing $|n|$ [8, 9, 10]. In contrast, when charge carriers are added into the bilayer sample, $\hbar\omega_G$ first decreases for smaller $|n|$ and then increases at larger doping (square symbols in Fig. 3b). As expected from the particle-hole symmetry in the system, two distinct minima are clearly resolved in $\hbar\omega_G(n)$. These minima indicate that G phonon stiffness changes from softening to hardening as carrier density increases.

Non-monotonic changes of phonon energy as a function of carrier density is quite unusual as it has never been observed before. In chemically doped silicon [19, 20] and EFE doped monolayer graphene [8, 9, 10], the phonon stiffness always changes monotonically with the carrier density. In this context, the double minima shown in Fig. 3b is quite anomalous. In the following, we ascribe that the observed minima are indeed manifestations of

the general phonon anomaly described in equation (1) above. First, we note the similarities between Fig. 1d and Fig. 3b, suggesting that the phonon energy minima correspond to $E_F = \pm \hbar\omega_G/2$ in bilayer graphene. Furthermore, between the two minima, the phonon line width (red dots in Fig. 3b) is larger than outside of the minima, indicating that Landau damping of the phonon into resonant electron-hole pair transition (blue arrows in Fig. 1a,b) is allowed within this region [8]. This is consistent with the fact that the anomaly positions correspond to the hole (left minimum) and the electron (right minimum) in the resonant electron-hole pair respectively.

Since the phonon anomaly can only occur at a special Fermi energy, charge density difference between these two minimal points $\Delta n_A \approx 6 \times 10^{12} \text{cm}^{-2}$ is linked to the electronic band parameters that determine the low energy dispersion of the bilayer graphene. Within the tight-binding model [23], we found from Δn_A the inter-layer $A_b - B_t$ hopping energy $\gamma_1 = 0.35 \pm 0.06 \text{eV}$. This value is in reasonable agreement with $\gamma_1 = 0.43 \pm 0.03 \text{eV}$ obtained from photoemission spectra in epitaxial bilayer graphene [24].

We expect the phonon anomaly to show up in single layer graphene if the sample quality is improved. In previous measurements [8, 11], single layer graphene samples contain large charge inhomogeneity, which yields electron and hole puddles of size $\delta n = 3 - 10 \times 10^{11} \text{cm}^{-2}$. This inhomogeneity corresponds to the mesoscopic Fermi energy broadening $\delta E_F \sim 100 \text{meV}$ near the Dirac point in single layer graphene, a value large enough to wash out the anomalous phonon softening completely. In bilayer graphene, however, similar δn results in much smaller

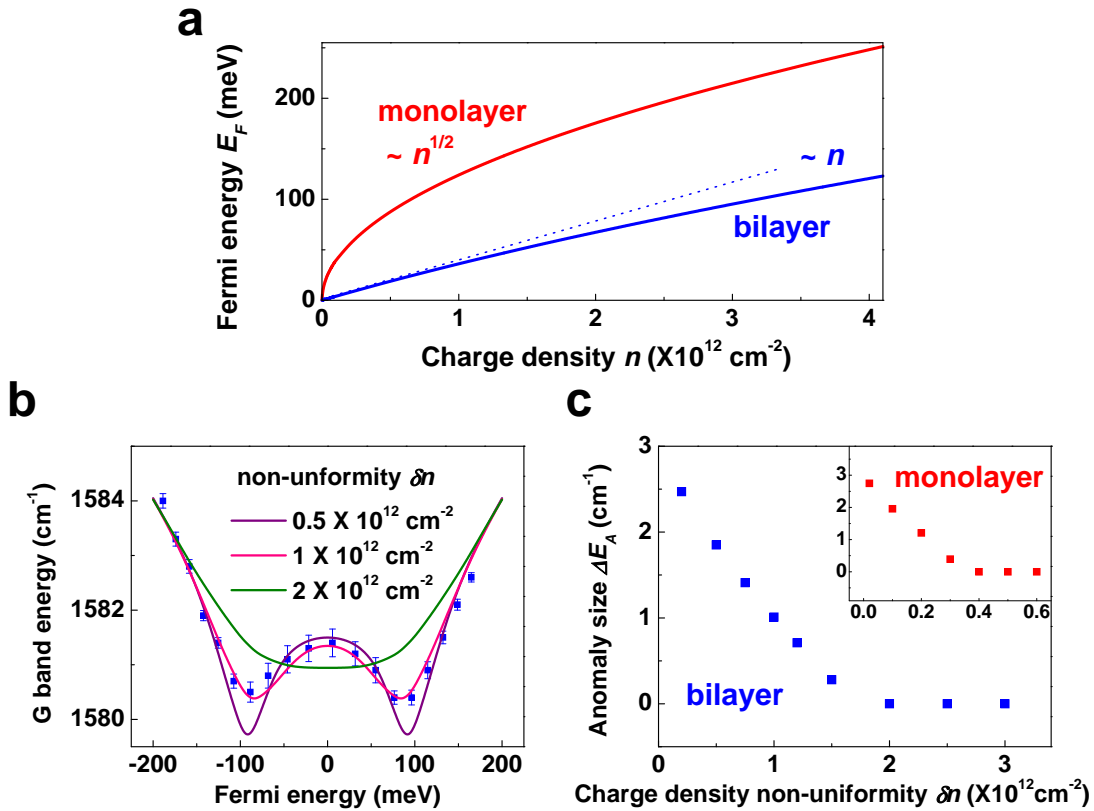


FIG. 4: **Broadening of the phonon anomaly by charge density non-uniformity.** **a**, Comparison of $E_F \sim n$ relation in bilayer and monolayer graphene. The Fermi energy goes up much faster with charge density in the monolayer. **b**, Fits of the evolution of the G phonon energy with E_F . The best fit has charge density non-uniformity $\delta n = 1 \times 10^{12} \text{ cm}^{-2}$. Blue squares are experimental data taken from Fig. 3b. **c**, Phonon anomaly ΔE_A as a function of charge density non-uniformity in the bilayer (main panel) and the monolayer (inset). The anomaly is more robust in bilayer graphene.

δE_F , because bilayer E_F changes much slower with n than the monolayer (n versus \sqrt{n} dependence in the low density regime), as shown in Fig. 4a. For this reason, the phonon anomaly is more robust and easier to observe in bilayer graphene.

To be more quantitative, we evaluated numerically the effect of charge inhomogeneity on $\hbar\omega_G(E_F)$, assuming a Gaussian distribution of the charge density $f(n) = \frac{1}{\sqrt{2\pi}\delta n} e^{-\frac{(n-n_0)^2}{2\delta n^2}}$, where n_0 is the average charge density in the sample, δn represents the size of the charge density non-uniformity. Figure 4b exemplifies several such evolutions for different δn . As expected, the larger δn is, the smaller is the phonon anomaly size $\Delta E_A = \hbar\omega_G(E_F=0) - \hbar\omega_G(E_F=\hbar\omega_G/2)$. Figure 4c displays ΔE_A as a function of δn . Comparing with the experimental observation, we estimate that $\delta n \approx 1 \times 10^{12} \text{ cm}^{-2}$ for $1 \text{ cm}^{-1} \Delta E_A$ in a bilayer. This size of charge density non-uniformity agrees well with results obtained from other experimental methods [25, 26, 27]. Note that similar size of charge density non-uniformity in single layer graphene is enough to smooth out the phonon anomaly completely (inset of Fig. 4c).

In conclusion, we have observed the anomalous soft-

ening of the long-wavelength optical phonon in bilayer graphene. This striking effect is a manifestation of the predicted logarithmic divergence due to tunable resonant coupling of phonons with particle-hole pairs. The broadening of the phonon anomaly is attributed to large charge density non-uniformity in graphene, showing that EFE-Raman spectroscopy can access fundamental interaction effects near the charge neutral point of graphene layers even in the presence of an inhomogeneous charge density distribution.

We thank I. Aleiner, D. Basko and A. Millis for helpful discussions. We acknowledge financial support from NSF (CHE-0117752), the NYSTAR, and ONR (N000140610138). P.K. acknowledges support from the FENA MARCO Center. A. P. is supported by NSF (DMR-0352738) and DOE (DE-AIO2-04ER46133).

Note added. - After completion of this work, we noticed a theoretical paper [28] on electron-phonon coupling in bilayer graphene, where it was confirmed that the long-wavelength optical-phonon energy again exhibits a logarithmic divergence as the charge density in the bilayer is continuously tuned.

-
- * Electronic address: jy2115@columbia.edu
- [1] Kohn, W. *Phys. Rev. Lett.* **2**, 393-394 (1959).
- [2] Novoselov, K.S. *et al. Science* **306**, 666-669 (2004).
- [3] Ando, T. *J. Phys. Soc. Jpn.* **75**, 124701 (2006).
- [4] Lazzeri, M. & Mauri, F. *Phys. Rev. Lett.* **97**, 266407 (2006).
- [5] Castro Neto, A. H. & Guinea, F. *Phys. Rev. B* **75**, 045404 (2007).
- [6] Saha, S. K., Waghmare, U. V., Krishnamurthy, H. R. & Sood, A. K. arXiv:cond-mat/0702627v2.
- [7] Basko, D. M. & Aleiner, I. L. arXiv:0709.1927v1.
- [8] Yan, J., Zhang, Y., Kim, P. & Pinczuk, A. *Phys. Rev. Lett.* **98**, 166802 (2007).
- [9] Pisana, S. *et al. Nature materials* **6**, 198-201 (2007).
- [10] Stampfer, C. *et al.* arXiv:0709.4156v1.
- [11] Yan, J., Zhang, Y., Goler, S., Kim, P. & Pinczuk, A. *Solid State Commun.* **143**, 39-43 (2007).
- [12] McCann, E., Abergel, D.S.L. & Fal'ko, V.I. *Solid State Commun.* **143**, 110-115 (2007).
- [13] Suzuura, H. & Ando, T. *Phys. Rev. B* **65**, 235412 (2002).
- [14] Ishikawa, K. & Ando, T. *J. Phys. Soc. Jpn.* **75**, 084713 (2006).
- [15] Mahan, G. D. *Many-Particle Physics* (Plenum, New York, 1990).
- [16] Wu, Y. *et al. Phys. Rev. Lett.* **99**, 027402 (2007).
- [17] Tsang, J. C., Freitag, M., Perebeinos, V., Liu, J. & Avouris, Ph. *Nature Nanotech.* **2**, 725-730 (2007).
- [18] Han, M., Özyilmaz, B., Zhang, Y., & Kim, P. *Phys. Rev. Lett.* **98**, 206805 (2007).
- [19] Chandrasekhar, M., Renucci, J. B. & Cardona, M. *Phys. Rev. B* **17**, 1623-1633 (1978).
- [20] Cerdeira, F. & Cardona, M. *Phys. Rev. B* **5**, 1440-1454 (1972).
- [21] Novoselov, K.S. *et al. Nature physics* **2**, 177-180 (2006).
- [22] Jiang, Z. *et al. Phys. Rev. Lett.* **98**, 197403 (2007).
- [23] McCann, E. & Falko, V. I. *Phys. Rev. Lett.* **96**, 086805 (2006).
- [24] Ohta, T., Bostwick, A., Seyller, T., Horn, K. & Rotenberg, E. *Science* **313**, 951-954 (2006).
- [25] Martin, J. *et al.* arXiv:0705.2180v1.
- [26] Tan, Y.-W. *et al.* arXiv:0707.1807v1.
- [27] Adam, S., Hwang, E. H., Galitski, V. M. & Das Sarma, S. arXiv:0705.1540v1.
- [28] Ando, T. *J. Phys. Soc. Jpn.* **76**, 104711 (2007).